# Change of confinement scale in nuclei: Predictions for structure functions confront electroproduction data

F. E. Close
*Rutherford Appleton Laboratory, Chilton, Didcot, Oxon OX11 OQX, United Kingdom*

R. L. Jaffe
*Center for Theoretical Physics, Laboratory for Nuclear Science, and Department of Physics, Massachusetts Institute of Technology, Cambridge, Massachusetts 02139*

R. G. Roberts
*Rutherford Appleton Laboratory, Chilton, Didcot, Oxon OX11 OQX, United Kingdom*

G. G. Ross
*Department of Theoretical Physics, University of Oxford, 1 Keble Road, Oxford, United Kingdom*

(Received 23 April 1984)

We confront our explanation of the "European Muon Collaboration effect," in which the quark confinement scale increases in going from a free nucleon to nucleus, with a new electroproduction experiment off several nuclear targets. The change of confinement size is attributed to the overlap of nucleons in nuclei which increases with nuclear density. A change of confinement scale modifies the quark and gluon distribution functions and we compute, in leading order in QCD, its effects for a series of different nuclei. New, precise electron scattering measurements at SLAC agree well with these predictions for $0.2<x<0.7$, supporting the postulate that the confinement size increases with nuclear density.

## I. INTRODUCTION

Recently it has become clear from experiments[1] probing nuclei at high momentum transfers that the conventional impulse description of a nucleus as a collection of protons and neutrons is incomplete. This began with the discovery[2] of the "European Muon Collaboration (EMC) effect" in the inelastic scattering of muons off iron. Even after standard corrections for Fermi-motion effects are made, the quark distributions in the range $5<Q^2<200$ GeV$^2$ disagree with those extracted from deuterium (essentially free nucleon). This discrepancy was independently confirmed[3] when similar phenomena were found in a reanalysis of old data where electrons were scattered off steel and aluminum targets.

The discrepancy largely disappears if the deuterium data at $Q^2$ are compared with iron data not at the same $Q^2$ but at $Q^2/2$ (Ref. 4), suggesting its origin may be due to a change in the intrinsic distance scale of the target. This agreed with the suggestion[4,5] that the effective confinement size of quarks and gluons in a nucleus is greater than in a free nucleon. Partial deconfinement could have been anticipated on several grounds: it is widely believed that even at zero temperature, nuclear matter undergoes a deconfining phase transition at some critical density $\rho_0$. At $\rho_0$, measures of the confinement length scale become large or even infinite, so it is not surprising that at densities below $\rho_0$ they exceed their values for the isolated nucleon. In the framework of perturbative QCD it was found that such a change in confinement scale predicts that nucleon and nuclear structure functions (at intermediate values of $x$) can be related by rescaling. That is, there exists a "rescaling parameter" $\xi_A(Q^2)$ determined by the change in confinement scale such that for nucleus $A$

$$\frac{1}{A}F_2^A(x,Q^2)=F_2^N(x,\xi_A(Q^2)Q^2)\ . \tag{1}$$

$\xi_A(Q^2)$ is in principle different for different moments. We show in Sec. II A, however, that in a valence-quark model $\xi_A(Q^2)$ is the same for all moments. The data agree well with this relation (1) when the confinement size in iron is 15% greater than in an isolated nucleon. This raises the question as to the source of the scale change and its expected $A$ dependence.

In Ref. 6 we proposed a model in which the change in confinement size is proportional to the probability that two nucleons overlap with one another. The QCD analysis was then applied with the predicted effective confinement size, $\lambda_A$, to give $\xi_A(Q^2)$ and, from Eq. (1), the quark distribution functions. These results are most directly compared with data in the form of ratios of structure functions on nucleus $A$ and deuterium. We calculated this ratio for fourteen nuclei and displayed[6] the result for particular values of $x$ and $Q^2$.

Subsequently the first data have been reported[7] for eight of these nuclei over a wide range of $x$ and $Q^2$. The predictions presented in Ref. 6 are reproduced here and confronted with these new data. The agreement is quite remarkable (cf. Figs. 2 and 3) throughout the range $0.2<x<0.7$. The purpose of this paper is to expand upon Ref. 6. We provide a detailed description of the model, confront its predictions with data, and suggest further tests.

## II. THE MODEL

Our analysis consists of two parts. First (Sec. II A), we describe how, in the context of perturbative QCD, quark and gluon distributions are modified by a change in scale of the target. The result is Eq. (1), together with a prediction of $\xi_A(Q^2)$ in terms of the change in confinement scale and an estimate of the ranges of $x$ and $Q^2$ over which it may be expected to hold. Second (Sec. II B), we construct a dynamical model for the rescaling parameter $\xi_A(Q^2)$. Of necessity, this step requires dynamical assumptions which go beyond asymptotic perturbative QCD.

### A. The effect of a change in confinement size

In this section we review the derivation of the rescaling relation, Eq. (1), from which the predictions for the nuclear dependence of the EMC effect follow. We consider the nuclear structure function $(1/A)F_2^A(x,Q^2)$ of a nucleus of atomic number $A$. We use Bjorken's definition of $x=Q^2/2M_p q^0$, so $x$ lies in the range $0\le x\le A$. The moments of the structure function are defined by

$$M_n^A(Q^2)=\frac{1}{A}\int_0^A dx\, x^{n-2}F_2^A(x,Q^2)\ . \tag{2}$$

They may be expressed in terms of an operator-product expansion

$$M_n^A(Q^2)/A^{n-2}=\frac{1}{Q^2}\sum_{n,i}C_{n,i}(Q^2,\mu_A{}^2)\bar{O}\,^A_{n,i}(\mu_A{}^2)\ , \tag{3}$$

where the summation is over all twist-two operators contributing to $F_2^A$. The $\bar{O}\,^A_{n,i}(\mu_A{}^2)$ are the reduced matrix elements of local operators normalized at the scale $\mu_A{}^2$,

$$\langle P\,|\,O^{A,i}_{\mu_1,\ldots,\mu_n}(\mu_A{}^2)\,|\,P\rangle=\bar{O}\,^A_{n,i}(\mu_A{}^2)P_{\mu_1}\cdots P_{\mu_n}\ . \tag{4}$$

If we are to relate the structure functions of different nuclei, at various $Q^2$, it is necessary to determine the nuclear dependence of the operator matrix elements at some initial scale. In the impulse approximation, a nucleus with atomic number $A$ is described by $A$ independent nucleons. This, with the normalization chosen in Eq. (3), would imply that $M_n^A(Q^2)$ be independent of $A$ and hence

$$A^{n-2}\bar{O}\,^A_{n,i}(\mu_A{}^2)=A'^{\,n-2}\bar{O}\,^{A'}_{n,i}(\mu_A{}^2)\ . \tag{5}$$

We want to modify this relation to take account of the possibility that different nuclei have different scales of confinement for the quarks and gluons. In a noninteracting-valence-quark approximation, the change in Eq. (5) is straightforward: quarks carrying momenta $p$ confined within a radius $\lambda$ simply transform to quarks carrying momenta $p'=(\lambda/\lambda')p$ when the scale of confinement is changed to $\lambda'$. There being no other scale in the system, the dimensionless quantity $p\lambda$ is constant.

We know that a simple valence-quark approximation for $F_2^A(x,Q^2)$ cannot apply for more than one value of $Q^2$, because radiative corrections modify the original valence-quark distribution, valid at $Q^2=\mu_0{}^2$, say, to give valence quarks plus gluon and quark bremsstrahlung at any other scale, $\mu_0'^2$. Remarkably it was found in deep-inelastic scattering that twist-two operator matrix elements are well approximated by a valence-quark (bag) model,[8] provided these operators are renormalized at a scale $\mu_0{}^2\approx 0.5$ GeV$^2$. Thus we consider it reasonable to use a simple valence-quark model, at this scale, to determine the modifications necessary to Eq. (5) to allow for a change in confinement size. This leads to the result

$$A^{n-2}\bar{O}\,^A_{n,i}(\mu_A{}^2)=A'^{\,n-2}\bar{O}\,^{A'}_{n,i}(\mu_{A'}{}^2)\ , \tag{6}$$

where

$$\mu_A{}^2=\mu_0{}^2 \ \text{ for } \ A=1 \tag{7}$$

and

$$\mu_{A'}{}^2=\left[\frac{\lambda_A{}^2}{\lambda_{A'}{}^2}\right]\mu_A{}^2\ . \tag{8}$$

In Eqs. (6)—(8) we have made the natural identification of $1/\lambda_A$, which determines a typical quark's momentum, with the renormalization scale $\mu_A$, of the quark fields from which the operators are constructed. This identification is supported by the fact that a change in the bag radius (i.e., $\lambda$) generates changes in valence-quark distribution functions which (approximately) mimic QCD evolution.[5] Equations (6)—(8) summarize our model for relating different nuclei. Obviously such relations would always be possible if the ratio $\mu_{A'}{}^2/\mu_A{}^2$ were allowed to be $n$ dependent (since the moments $M_n^A(Q^2)$ are monotonically decreasing with $Q^2$); the nontrivial content of these equations is that $\mu_A{}^2$ and $\mu_{A'}{}^2$ should be independent of $n$. This will occur in any model in which quark-momentum distribution depends on only one dimensionful parameter (for example, the bag radius in the bag model) and is the simplest possibility we can imagine. We can gain some insight into the physics of the initial condition of Eqs. (6)—(8) by noting that the difference between the matrix elements $\bar{O}\,^A_{n,i}(\mu_A{}^2)$ and $\bar{O}\,^A_{n,i}(\mu_{A'}{}^2)$ may be calculated, in QCD, by computing the bremsstrahlung of quarks and gluons. In leading order this gives

$$\bar{O}\,^A_{n,i}(\mu_{A'}{}^2)-\bar{O}\,^A_{n,i}(\mu_A{}^2)=\frac{\alpha_s}{8\pi}\gamma_0^n\int_{\mu_{A'}{}^2}^{\mu_A{}^2}\frac{dk_T{}^2}{k_T{}^2}\bar{O}\,^A_{n,i}(\mu_{A'}{}^2)\ , \tag{9}$$

where the integral runs over the transverse momentum squared of the bremsstrahled gluon and $\gamma_0^n$ is the familiar anomalous dimension, in leading order. Thus the difference between the operators normalized at different scales corresponds to adding the bremsstrahled gluons (and quarks) whose momenta extend over the phase space between the scales $\mu_{A'}{}^2$ and $\mu_A{}^2$. This makes a direct connection with Eq. (8) because increasing the confinement size requires us to add the contribution of gluons (and quarks) which can propagate to the new boundary, of radius $\lambda_{A'}$, before feeling the effects of confinement. This corresponds to adding gluons with momenta between $\lambda_{A'}{}^{-1}$ and $\lambda_A{}^{-1}$ in agreement with Eq. (9) with $\mu_A{}^2$ and $\mu_{A'}{}^2$ given by Eq. (8).

Note that Eq. (6) remains true even if we include the leading-order QCD correction, as in Eq. (9). It applies to any value of $\mu_A{}^2$. Once we use the renormalization-group equations to resum the leading-logarithmic corrections and to express Eq. (9) in terms of the running coupling constant, Eq. (9) becomes

$$\bar{O}^{A}_{n,i}(\mu_A{}^2)=\left[\frac{\alpha_s(\mu_A{}^2)}{\alpha_s(\mu_{A'}{}^2)}\right]^{-d_n}\bar{O}^{A}_{n,i}(\mu_{A'}{}^2)\ , \tag{10}$$

where

$$d_n=\gamma_0^n/2\beta_0 \tag{11}$$

and

$$\alpha_s(Q^2)=4\pi/[\beta_0\ln(Q^2/\Lambda_{\rm QCD}{}^2)]\ . \tag{12}$$

We have argued that Eq. (6) should be true for a unique value of $\mu_A{}^2$, with $\mu_{A'}{}^2$ given by Eq. (8). This value is the scale at which the valence-quark approximation works well for the twist-two operator components and is expected to be of order of a hadronic mass scale. Indeed, from Eqs. (10) and (12) we see explicitly that Eqs. (6) and (8) can be true for only a unique scale, for the left- and right-hand sides of Eq. (6) change by different, $n$ dependent amounts on changing $\mu_A{}^2$ and $\mu_{A'}{}^2$ while keeping $\mu_A{}^2/\mu_{A'}{}^2$ fixed. Thus we see why we have given a physical interpretation to the operator renormalization scale. Normally this is arbitrary and can be changed if one simultaneously changes it in the coefficient functions. In this case, however, Eq. (6) is true only for a specific choice of renormalization point, i.e., only for a specific definition of the operator defined at the unique scale where the twist-two component of the nucleus is given by valence quarks alone.

We turn now to the use of Eqs. (6)—(8) to relate the structure functions of different nuclei. For large $Q^2$, the coefficient functions of Eq. (3) may be calculated perturbatively in QCD giving, in leading-logarithmic order,

$$M_n^A(Q^2)=\left[\frac{\alpha_s(Q^2)}{\alpha_s(\mu_A{}^2)}\right]^{d_n}M_n^A(\mu_A{}^2)\ . \tag{13}$$

Using Eq. (6), we find

$$\begin{aligned}M_n^{A'}(Q^2)&=\left[\frac{\alpha_s(Q^2)}{\alpha_s(\mu_{A'}{}^2)}\right]^{d_n}M_n^A(\mu_A{}^2)\\&=M_n^A(\xi_{AA'}(Q^2)Q^2)\ ,\end{aligned} \tag{14}$$

where

$$\xi_{AA'}(Q^2)=\left[\frac{\lambda_{A'}{}^2}{\lambda_A{}^2}\right]^{\alpha_s(\mu_{A'}{}^2)/\alpha_s(Q^2)}\ . \tag{15}$$

In deriving this equation we have used the result

$$\alpha_s{}^{-1}(\mu_{A'}{}^2)=\frac{\beta_0}{4\pi}\ln\left[\frac{\mu_{A'}{}^2}{\mu_A{}^2}\right]+\alpha_s{}^{-1}(\mu_A{}^2) \tag{16}$$

to show that

$$\frac{\alpha_s(Q^2)}{\alpha_s(\mu_{A'}{}^2)}=\frac{\alpha_s(\xi Q^2)}{\alpha_s(\mu_A{}^2)}\ . \tag{17}$$

Since $\xi_{AA'}(Q^2)$ is independent of $n$ we get the rescaling relation

$$\frac{1}{A'}F_2^{A'}(x,Q^2)=\frac{1}{A}F_2^A(x,\xi_{AA'}(Q^2)Q^2)\ . \tag{18}$$

This concludes our derivation, to leading order, of the effects of a change of confinement size on the twist-two nuclear structure functions. Before we confront experiment with this dynamical rescaling, let us consider the accuracy we may expect. There are two types of correction to the form of Eq. (18), following from nonleading QCD corrections and from higher-twist corrections. The latter are suppressed by inverse powers of $Q^2$ and may be expected to be small, except at the end points of the $x$ range. The former, however, involve corrections suppressed only by $\alpha_s(\mu^2)$ where $\mu^2$ may be below 1 GeV$^2$. They could be quite large and it is important therefore to check them in detail. Note that though our analysis continues to low $\mu^2$, this is only done to relate the twist-two operators. Twist $>2$ are still suppressed by powers of $Q^{-2}$ relative to leading twist, where $Q^2$ is the point at which the structure function is measured.

In Ref. 8, an analysis was made of the second-order QCD corrections to nonsinglet moments using a value for $\mu_0{}^2=0.75$ GeV$^2$ and $\Lambda_{\overline{\rm MS}}=250$ MeV ($\overline{\rm MS}$ denotes the modified minimal-subtraction scheme). Although $\bar{\alpha}(\mu_0{}^2)$ is quite large, it was found that substantial ($>50\%$) next-to-leading-order corrections to Eq. (14) occurred only for $n=2$ and $n>8$. For intermediate values of $n$, $2<n<10$, the coefficients of the second-order terms were small, supporting our use of leading-order QCD to derive Eq. (1).

In order to determine the $x$ range of validity of our first-order QCD predictions it is necessary to invert the moments to determine where the large second-order corrections to the $n=2$ and $n>8$ moments will be significant. This can be done using a second-order Altarelli-Parisi analysis of the $Q^2$ evolution structure functions for different nuclei with the initial condition [corresponding to Eq. (6)]

$$\frac{1}{A}F_2^A(x,\mu_A{}^2)=\frac{1}{A'}F_2^{A'}(x,\mu_{A'}{}^2)\ . \tag{19}$$

However, this analysis is numerically complicated and has not been performed. Instead we give a qualitative answer to the question. For small $x$, the effective value of $n$ dominating the inverse Mellin transform is approximately given by[9]

$$(n-1)\simeq[\,|\ln\alpha_s/\ln x\,|\,]^{1/2}\ , \tag{20}$$

so $n=2$ corresponds, roughly, to $x=\alpha_s$. For large $x$, the dominant value of $n$ is

$$n\simeq\ln\alpha_s/\ln x \tag{21}$$

which, for $n=10$, gives $x\simeq\alpha_s{}^{1/2}$. For $\alpha_s\simeq0.2$ the range of validity is of the order

$$0.2<x<0.9\ .$$

The second-order corrections considered, so far, are those modifying Eq. (14). In deriving Eq. (1) from Eq. (14) we used the expansion of Eq. (16) for $\alpha_s{}^{-1}(\mu_A{}^2)$. Thus we must also consider the second-order corrections to $\alpha_s{}^{-1}$.

This leads to the corrected form of the rescaling parameter,

$$\xi_{AA'}(Q^2)=\left[\frac{\lambda_{A'}^2}{\lambda_A^2}\right]^{\alpha_s(\mu_{A'}^2)/\alpha_s(Q^2)}\times\left[\frac{\alpha_s(\mu_{A'}^2)}{\alpha_s(\mu_A^2)}\right]^{(\beta_1/\beta_0^2)[\alpha_s(\mu_{A'}^2)-\alpha_s(Q^2)/\alpha_s(Q^2)]} \tag{22}$$

For $\lambda_{A'}>\lambda_A$ this modification increases the one-loop estimate for $\xi$ only slightly. For example, with $\lambda_{A'}/\lambda_A=1.15$, $\xi_{AA'}$ is increased by less than 7%.

### B. The $A$ dependence of the quark confinement scale

In order to estimate the $A$ dependence of the rescaling parameter $\xi_{AA'}$ we construct a simple model for the partial deconfinement of quarks within the nucleus. In short, we assume quarks to be deconfined to an extent proportional to the amount that nucleons within the nucleus overlap. When nucleons overlap, we assume that their quarks are free to propagate over a larger spatial domain. To measure the overlap of nucleons we treat them as spheres of constant density and radius $a$. For any two nucleons the overlapping volume (measured in units of the nucleon volume) is

$$V_0\left[\frac{d}{a}\right]=\begin{cases}1-\frac{3}{4}\left[\frac{d}{a}\right]+\frac{1}{16}\left[\frac{d}{a}\right]^3, & d\le 2a,\\ 0, & d\ge 2a,\end{cases} \tag{23}$$

where $d=|\mathbf{r}_1-\mathbf{r}_2|$. The radius $a$ is chosen so that the rms radius of a sphere of constant density equals the rms radius of the nucleon, $a_{\rm rms}$. This fixes $a=(\frac{5}{3})^{1/2}a_{\rm rms}$.

In a nucleus with $A$ nucleons, any given nucleon may overlap with $(A-1)$ others. If the nucleons are distributed according to some two-particle density function $\rho_A(\mathbf{r}_1,\mathbf{r}_2)$, then the overlapping volume per nucleon is

$$V_A=(A-1)\int d^3\mathbf{r}_1 d^3\mathbf{r}_2\,\rho(\mathbf{r}_1,\mathbf{r}_2)V_0(|\mathbf{r}_1-\mathbf{r}_2|/a)\,, \tag{24}$$

where the function $\rho_A(\mathbf{r}_1,\mathbf{r}_2)$ is normalized to unity, i.e.,

$$\int d^3\mathbf{r}_1 d^3\mathbf{r}_2\,\rho_A(\mathbf{r}_1,\mathbf{r}_2)=1\ .$$

We replace $\rho_A(\mathbf{r}_1,\mathbf{r}_2)$ by the product of single-particle densities $\rho_A(r_1)$ (normalized to unity), $\rho_A(r_2)$ and the two-nucleon correlation function $F_A(|\mathbf{r}_1-\mathbf{r}_2|)$. Nuclear densities saturate at large $A$ and so $\rho_A\sim 1/A$. Consequently, despite the explicit factor $(A-1)$ in Eq. (24) we find that $V_A$ saturates, i.e., $V_A\to$constant, for large $A$.

We assume the nuclear-density function $\rho_A(r)$ has the same shape as the charge-density function which we take from nuclear-structure tables. This we believe to be valid for $A\le 40$. For $A>40$ the nuclear density is somewhat smoother than the charge density,[10] so we do not take so seriously the small fluctuations in $V_A$ for large $A$. Not surprisingly it is this density function which dictates the $A$ dependence of the nuclear structure functions: the more densely packed the nucleons, the greater likelihood there is for overlap. For nucleons separated by less than about 1 fm, some modification of the two-nucleon density is expected and this is described by the correlation function $F_A(|\mathbf{r}_1-\mathbf{r}_2|)$. The $A$ dependence of $F_A$ is unknown except for simple models of the simplest nuclei. We therefore approximate $F_A$ by $F_\infty$, the two-nucleon correlation function for nuclear matter. We try to investigate sensitivity to the short-distance separation by varying the choice of the correlation function. We consider three possibilities.

(a) No correlation, i.e.,

$$\rho_A(\mathbf{r}_1,\mathbf{r}_2)=\rho_A(\mathbf{r}_1)\rho_A(\mathbf{r}_2)$$

or

$$F(r)=1\ .$$

(b) Correlations arising from treating the constituent nucleons as a Fermi gas,

$$F(r)=1-\tfrac{1}{4}[3j_1(k_Fr)/(k_Fr)]^2\ ,$$

where $k_F$, the Fermi momentum, $\sim$250 MeV.

(c) Correlations which follow from describing the two-nucleon force by the Reid soft-core potential.[11] This is probably the most sophisticated correlation we can attempt.

These three correlation functions are compared in Fig. 1. Notice that the correlations (b) and (c) reduce the probability of two nucleons approaching closely. Since this is when overlap will be greatest, the effect of introducing correlations is to reduce the deconfinement of quarks.

The effective confinement size $\lambda_A$ in a nucleus of atomic number $A$ will then be intermediate between $\lambda_N$, the confinement size for an isolated nucleon, and $\lambda_{\rm tot}$, the confinement size associated with two totally overlapping nucleons. The relative weighting between $\lambda_N$ and $\lambda_{\rm tot}$ is governed by the probability for overlap, $V_A$, and so we expect $\lambda_A$ to be given by interpolation,

$$\frac{\lambda_A}{\lambda_N}=1+V_A\left[\frac{\lambda_{\rm tot}}{\lambda_N}-1\right]. \tag{25}$$

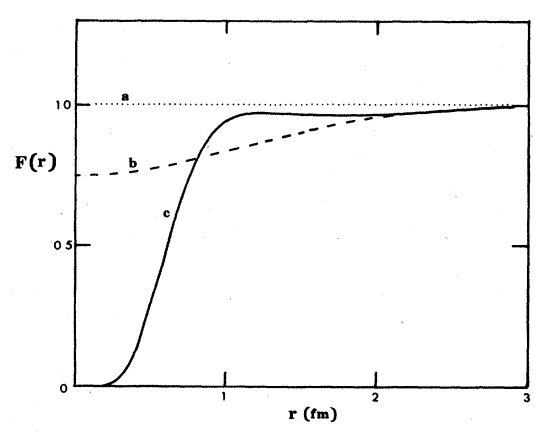


FIG. 1. Correlation function $F(r)$ between two nucleons separated by distance $r$. (a) no correlation, (b) Fermi-gas model $F(r)=1-\frac{1}{4}[3j_1(k_Fr)/k_Fr]^2$, (c) Reid soft-core potential.

TABLE I. Values of the confinement size relative to that for the free nucleon for a range of nuclei. The three values (a), (b), and (c) correspond to the three choices of the correlation function $F(r)$.

| Nucleus | | $\lambda_A/\lambda_N$ | |
|---|---|---|---|
| | (a) | (b) | (c) |
| $^2$D | 1.018 | 1.015 | 1.015 |
| $^3$He | 1.047 | 1.042 | 1.040 |
| $^4$He | 1.092 | 1.082 | 1.079 |
| $^6$Li | 1.054 | 1.045 | 1.045 |
| $^7$Li | 1.075 | 1.064 | 1.063 |
| $^9$Be | 1.088 | 1.074 | 1.074 |
| $^{12}$C | 1.124 | 1.105 | 1.104 |
| $^{16}$O | 1.128 | 1.109 | 1.108 |
| $^{20}$Ne | 1.122 | 1.104 | 1.104 |
| $^{27}$Al | 1.165 | 1.140 | 1.140 |
| $^{32}$S | 1.157 | 1.134 | 1.134 |
| $^{40}$Ca | 1.161 | 1.137 | 1.137 |
| $^{48}$Ca | 1.196 | 1.166 | 1.166 |
| $^{56}$Fe | 1.180 | 1.153 | 1.154 |
| $^{63}$Cu | 1.181 | 1.154 | 1.154 |
| $^{107}$Ag | 1.198 | 1.168 | 1.169 |
| $^{118}$Su | 1.205 | 1.175 | 1.176 |
| $^{197}$Au | 1.229 | 1.196 | 1.195 |
| $^{208}$Pb | 1.220 | 1.188 | 1.188 |

TABLE II. Values of the rescaling parameter $\xi_{AA'}$ for $A'=2$ at $Q^2=20$ GeV$^2$ using the Reid soft-core version of the correlation function.

| Nucleus | $\xi_A(Q^2=20)$ |
|---|---|
| $^2$D | 1.07 |
| $^3$He | 1.20 |
| $^4$He | 1.43 |
| $^6$Li | 1.23 |
| $^7$Li | 1.33 |
| $^9$Be | 1.40 |
| $^{12}$C | 1.60 |
| $^{16}$O | 1.63 |
| $^{20}$Ne | 1.60 |
| $^{27}$Al | 1.89 |
| $^{32}$S | 1.84 |
| $^{40}$Ca | 1.86 |
| $^{48}$Ca | 2.14 |
| $^{56}$Fe | 2.02 |
| $^{63}$Cu | 2.02 |
| $^{107}$Ag | 2.17 |
| $^{118}$Sn | 2.24 |
| $^{197}$Au | 2.46 |
| $^{208}$Pb | 2.37 |

The ratio $\lambda_{\rm tot}/\lambda_N$ is taken to be $2^{1/3}$ which follows if the total overlap volume of two nucleons is simply twice the volume of a single nucleon. With this choice of $\lambda_{\rm tot}/\lambda_N$, the values of $\lambda_A/\lambda_N$ were then calculated for each nucleus from Eqs. (24) and (25) and then fed into Eq. (15) for the rescaling parameter.

We have neglected multiple overlap between three or more nucleons, which is certainly justified if the probability for two-nucleon overlap is small. Even when the two-nucleon overlap is not small our procedure turns out to be reliable because the resulting overestimate of the two-nucleon overlap is approximately compensated by the neglect of the three- (or multiple-) nucleon overlap. An example of how this occurs is shown in Appendix B. Since the $A$ dependence of the effective confinement size $\lambda_A$ is determined by the $A$ dependence of the nucleon-density function, it is clear that $\lambda_A$ will reach a maximum value as the nucleon density saturates. As we will discuss in the next section, this saturation value corresponds to an increase of confinement size of 20% over that of an isolated nucleon.

## III. COMPARISON WITH DATA

Using the model described in Sec. II we made predictions for the nuclear dependence of the structure function. In this section we compare those predictions with the recent SLAC electroproduction experiment[7] using nine nuclear targets.

First some remarks about parameters. We have four quantities which could be regarded as parameters but there is independent information which gives a preferred value in each case.

(i) *The rms radius of the nucleon,* $a_{\rm rms}$. This controls the degree of overlap of nucleons which, in turn, determines the confinement size $\lambda_A$ in the nucleus. Experimentally the rms charge radius of the proton is well determined to be $0.88\pm0.03$ fm (Ref. 12) and we take $a_{\rm rms}=0.9$ fm.

(ii) *The scale* $\mu_A{}^2$. That is where the structure function is taken to be the initial valence-quark distribution, with no radiated gluons. This scale can be fixed by examining the $Q^2$ dependence of the experimental nonsinglet structure functions and comparing with the bag structure function in the method of Jaffe and Ross.[8] In the Appendix we update this procedure and find $\mu_{A=56}{}^2=0.50\pm0.11$ GeV$^2$, which corresponds to $\mu_{A=1}{}^2=0.66\pm0.14$ GeV$^2$.

(iii) *The QCD scale parameter* $\Lambda_{\rm QCD}$. This controls the $Q^2$ variation of $\alpha_s(Q^2)$ and is determined from analyzing the scaling violations of structure functions. Recent evaluations[13,14] give $\Lambda_{\overline{\rm MS}}=250\pm100$ MeV.

(iv) *The ratio* $\lambda_{\rm tot}/\lambda_N$. As stated in the last section, we take this to be $2^{1/3}$ which follows from volume invariance of the two-nucleon system. However this value can be justified from bag-model considerations. In the bag model a virial theorem relates the mass and volume of hadrons containing only light quarks; $M=4BV$. Since the nonstrange six-quark bag system is not bound, $M_{(6)}>2M_{(3)}$ and we expect that $R_{(6)}>2^{1/3}R_{(3)}$.

When we discussed the original EMC effect, for data off an iron target, we found that the data were consistent with the rescaling hypothesis for the choice $\xi_{A=56}\simeq2$. The values of the four quantities above result in exactly this value for the rescaling parameter which gives us confidence that our approach is a reasonable one. We discuss the sensitivity of our predictions to these parameters further on.

Table I shows the values of $\lambda_A/\lambda_N$ obtained with each choice of correlation function. As expected, the choices (b) and (c) yield a smaller confinement size. Also we see that approximating deuterium by a free nucleon is acceptable. For heavy nuclei, we notice that the confinement size is 20% larger than for a free nucleon. Taking the Reid soft-core correlation function, the resulting values for the rescaling parameter $\xi_{AA'}(Q^2)$ at $Q^2=20$ GeV$^2$ and $A'=2$ are listed in Table II. In order to make predictions for the new SLAC experiment we ensure that $\xi_{AA'}(Q^2)$ is computed at the value of $Q^2$ relevant to each measurement of $F_2^A(x,Q^2)$.

Finally, in order to exploit the rescaling expression, Eq. (18), we must know the $Q^2$ behavior of the deuterium structure function. This is provided by the EMC measurements of $F_2^D(x,Q^2)$.[15] Since we need to interpolate to any desired value of $x$ and $Q^2$, we have carried out a QCD fit to these data and insert these values into the right-hand side of Eq. (18). Incidentally, this fit yields a value of $\Lambda_{\rm QCD}$ consistent with our choice above.

Our analysis applies to the ratio of structure functions $F_2^A(x,Q^2)/F_2^D(x,Q^2)$. Arnold *et al.*[7] present instead the ratio $\sigma^A/\sigma^D$. The two can differ if $R=\sigma_L/\sigma_T$ is $A$ dependent and is not negligibly small. The framework of our model is leading-order QCD in which $R$ is zero. So we compare our calculated ratio of structure functions directly with the SLAC data. The possibility that $R$ is large and $A$ dependent and helps to reconcile the superficial difference between SLAC and EMC data at low $x$ is discussed further in Sec. IV. Figure 2 shows the predicted $A$ dependence of $F_2^A(x,Q^2)/F_2^D(x,Q^2)$ at a fixed value of $x$ (and $Q^2$). The roughly logarithmic dependence in both the experimental points and our predictions is consistent with the general slow increase of nucleon density with increasing $A$. We also show the prediction which follows from taking a smooth interpolation of nucleus radius. For that we take a Gaussian distribution

$$\rho_A(r)=[3/(2\pi R_A{}^2)]^{3/2}\exp[-3r^2/(2R_A{}^2)] \qquad (26)$$

with

$$R_A=0.84A^{1/3}\,0.6\ .$$

It can be seen that the curve roughly interpolates the predicted points. Fluctuations about the smooth behavior therefore represent fluctuations of the nucleon density and are probably only significant at small $A$. At large $A$, the neutron-density function is not the same as the proton density and tends to smooth out such fluctuations.[10] For light nuclei, however, the deviations from smooth $A$ dependence are genuine. In particular, our predictions reflect the "above the trend" density of $^4$He and "below the trend" density of $^9$Be resulting in approximately equal structure functions for these two nuclei. The data of the SLAC experiment confirm this behavior, thus indicating that the nuclear dependence of the structure functions is indeed dictated by the nucleon density. Data on $^6$Li would be very interesting to compare with $^4$He and $^9$Be as we predict $^6$Li to show considerably less of an effect than its neighbors—see Fig. 4. Comparison with $^3$He would highlight the anomalous case of $^4$He. $^{48}$Ca is anomalously dense compared to its immediate neighbors. In fact, we expect the structure function of $^{48}$Ca and $^{107}$Ag to be similar in magnitude.

The relative $x$ dependences of nuclear structure functions are governed by the pattern of $Q^2$ scaling violations of the deuterium structure function. Figure 3 shows the $x$

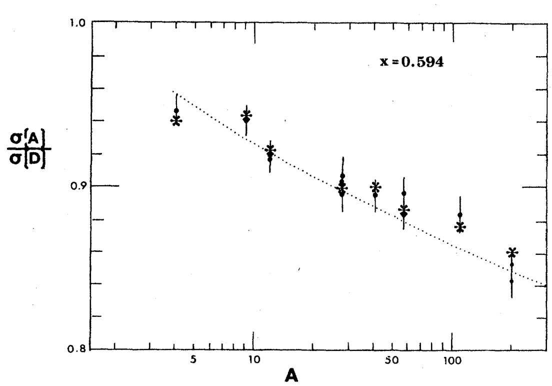


FIG. 2. SLAC data (Ref. 7) on the $A$ dependence of the ratio of electroproduction cross sections, $\sigma(A)/\sigma$ (D), denoted by ●, together with our predictions, denoted by $*$, at fixed $x$ (0.594) and $Q^2=4.98$ GeV$^2$. $\sigma_L/\sigma_T$ has been assumed to be independent of $A$. The dotted curve indicates the result of approximating the nucleon density with a smooth $A$-dependent Gaussian function.

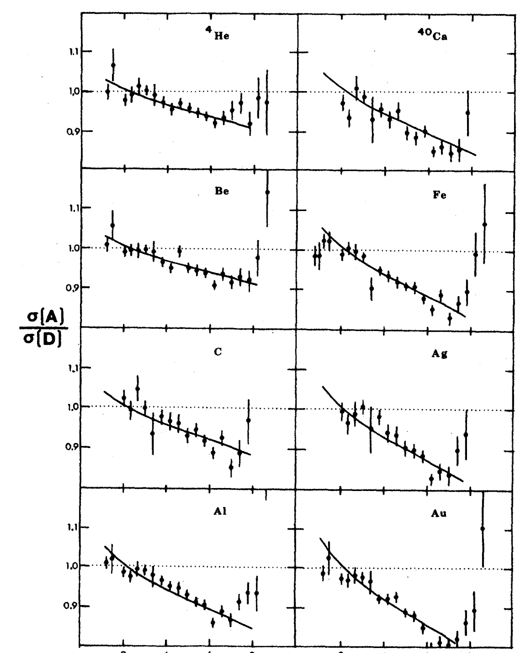


FIG. 3. Comparison of the $x$ dependence of the ratio of electroproduction cross sections, $\sigma(A)/\sigma$(D), between our predictions (denoted by the solid curves) and the SLAC data (●) averaged over $Q^2$. Our predictions use $Q^2$ values given by $Q^2=16.x$ GeV$^2$. The eight nuclei correspond to $A=4$, 9, 12, 27, 40, 56, 107, and 197.

dependence of $F_2^A(x,Q^2)/F_2^D(x,Q^2)$ for eight values of $A$, compared with the SLAC experiment. As before the $A$ dependence of $\sigma_L/\sigma_T$ is assumed to be insignificant. Over this wide range of nuclei, the agreement between our predictions and the SLAC data is excellent over the range $0.2 \le x \le 0.7$.

We have investigated the systematic effects resulting from varying the parameters ${\mu_{A=1}}^2$ and $\Lambda_{\overline{\rm MS}}$ within their uncertainties (0.11 GeV$^2$ and 100 MeV, respectively). To a very good approximation, the result is a systematic shift of all the points in Fig. 2 by a maximum of 3.5%. The same effect is generated by alternatively varying the free parameter $a_{\rm rms}$ by 0.1 fm, demonstrating that it is this parameter to which the results are most sensitive. In this context, there is a definite preference for a two-nucleon correlation, like the Reid soft-core function, which suppresses close proximity of nucleons in the nucleus. Ignoring this correlation would lead to a high degree of overlap unless it was compensated by a value for the nucleon radius significantly below the range allowed by the experimental determination of $a_{\rm rms}$.

## IV. DISCUSSION AND CONCLUSIONS

Our view is that the source of the EMC effect is the fact that the confinement size for quarks in nuclei is larger than in free nucleons. We have shown that QCD then leads to a rescaling relation, Eq. (1), which says that altering the confinement scale at a fixed value of $Q^2$ is equivalent to altering the value of $Q^2$ for a given target. The $Q^2$ dependence is just the well known pattern of scaling violations due to radiation of gluons. Indeed a partial deconfinement is not entirely unexpected and several other authors[16–18] have realized the connection between this and the EMC effect. The typical increase in confinement scale we believe to be around 15%, in contrast, to the suggestion of Nachtmann and Pirner,[16] where the quark confinement scale is of the order of the nuclear radius.

We made the further assumption that the expansion in the confinement scale arises from the overlap of nucleons in the dense nucleus. To compute the $A$ dependence of the confinement size we used a geometrical calculation of the overlap volume, an assumption which can be motivated in the bag model. However this really requires deeper justification—the detailed nuclear dynamics which produce the change of confinement size may involve clusters inside the nucleus,[5,17,19–22] the presence of pions[23–25] or $\Delta$'s[26] in the nucleus.

As a consequence of our approach of considering directly the quark distributions in the nucleus, the structure functions for any pair of nuclei can be equated by rescaling, at least within a limited $x$ range. The magnitude of the rescaling parameter $\xi_{AA'}$ is controlled by the relative confinement sizes within the two nuclei, which in turn is driven by the difference in nuclear densities. Nevertheless, as our comparison with the SLAC data shows, any model which correlates $\xi_{AA'}$ with the nuclear density is bound to succeed in describing the $A$ dependence of the effect.

It should be noted that the shift $\xi_{AA'}$ depends on $Q^2$. The values listed in Table II correspond to $Q^2=20$ GeV$^2$, and the values of $\xi_{AA'}$ relevant to the SLAC data ($Q^2=2$–15 GeV$^2$) are, of course, smaller than for the EMC data ($Q^2=10$–200 GeV$^2$). An investigation has been carried out by Liu, Li, and Liu,[27] who demonstrate that the SLAC data indeed satisfy rescaling but with $\xi_{\rm iron}^{\rm SLAC} < \xi_{\rm iron}^{\rm EMC}$. Our initial analysis[4] of the EMC data showed consistency with dynamical rescaling (with $\xi_{\rm D,Fe} \approx 2$) except for $x < 0.2$. This is evident from Fig. 4 where we plot the ratio of iron/deuterium structure functions measured by EMC[2] compared with the result of our model. Also shown are the preliminary data of the BCDMS collaboration.[28] If we take our QCD fit to the EMC deuterium data,[15] and ask how well dynamical rescaling describes the EMC iron data[29] we find a $\chi^2$ of 147 for 175 data points if $\xi=2$, over the entire $x$ range. The agreement with dynamical rescaling is further improved if one allows for a 4% reduction in the normalization of the iron data relative to the deuterium data. Such a shift is well within the quoted normalization uncertainty and is strongly hinted at by the new BCDMS data. In any case, we do not claim our leading-logarithm approximation to be realistic at small $x$, and a discrepancy there is not a serious blow.

The failure of the SLAC data to confirm the EMC observation of an enhancement at low $x$ may be attributed to the low values of $Q^2$ where the SLAC low-$x$ data are taken. Higher-twist effects like shadowing are expected to be important at low $x$ and could account for the difference. Such effects together with the effects of Fermi

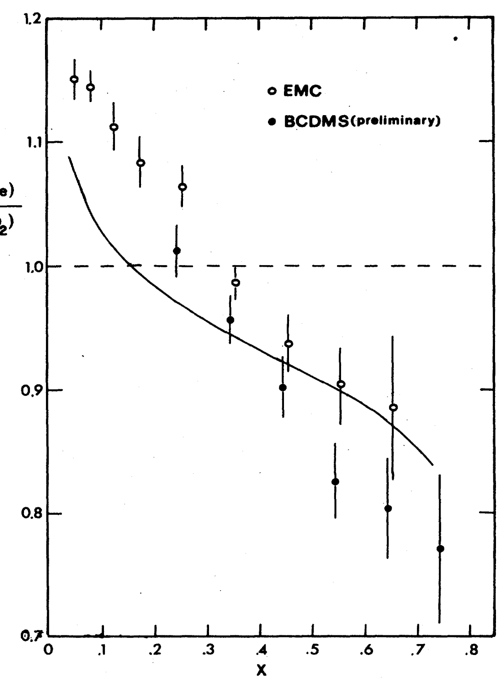


FIG. 4. Ratio of structure functions iron/deuterium in muoproduction. The curve corresponds to our model and the data is from the NA2 and NA4 experiments at CERN (Refs. 2 and 28).

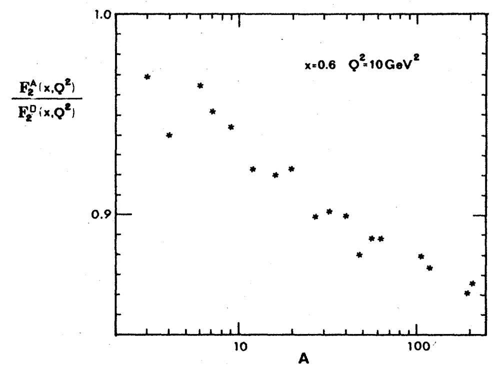


FIG. 5. Predictions for $F_2^A(x,Q^2)/F_2^{\rm D}(x,Q^2)$ for the full range of nuclei listed in Tables I and II, at $x=0.6$, $Q^2=10$ GeV$^2$.

motion (at large $x$), and other higher-order or higher-twist corrections to nuclear structure functions are outside of our leading-twist, leading-order QCD analysis.

One point which arises in a discussion of both the EMC and SLAC data is the question of $R=\sigma_L/\sigma_T$, and in particular its $A$ dependence. The EMC used a value of $R=0$ in converting their cross sections off deuterium and iron into values of $F_2$, while SLAC simply present the ratio of the cross sections. Clearly the two ratios are equal provided $R$ is independent of $A$. Indeed Arnold *et al.*[7] measured $R$ for three of their targets for $Q^2=5$ GeV$^2$. While it is not surprising that these values are not zero at such low $Q^2$, the relevant issue is whether they vary with $A$ at each value of $x$. Averaged over $x=0.3$, 0.5, 0.7 there is a hint of a small rise with increasing $A$, although the errors are such that the results could be consistent with independence of $A$. The framework of our model is leading-order QCD in which $R$ is zero. Even $O(\alpha_s)$ computation of $R$ gives a very small value for $x>0.2$, substantially smaller than the measurements off proton targets.[30] The most likely origin of significantly nonzero values at small $Q^2$ is higher-twist terms[31,32] which therefore lie outside the scope of our present approach. If it eventually turns out that $R$ depends significantly on $A$, then a more careful combined analysis of the two sets of data will be necessary.

The SLAC data incidentally covers a range of $Q^2$ which reaches down to 2 GeV$^2$ and it might seem that the agreement shown in Fig. 3 is far better than we had a right to expect, in view of our neglect of higher-twist terms. The data plotted in Figs. 2 and 3, however, are $Q^2$- averaged values at each $x$. In Sec. II A we argued that to avoid possible higher-order corrections we should keep $x>0.2$ and for such values of $x$ the SLAC range of $Q^2$ is $2\rightarrow 10$ GeV$^2$, with $\langle Q^2\rangle \approx 5$ GeV$^2$. Experimentally we know that structure functions can be successfully described in terms of only leading-twist contributions[13,14] for $Q^2>4$ GeV$^2$, and so we may be fairly safe with our asymptotic model provided $0.2<x<0.8$. Again this may be true as long as $F_2$ is dominated by $\sigma_T$; as we mentioned above, $\sigma_L$ could be entirely higher twist.

Finally, we list some features which further experiments could profitably explore.

(1) Our knowledge of the low-$x$ region of the EMC effect is incomplete. EMC measured $F_2^{\rm Fe}/F_2^{\rm D}$ at low $x$ for $Q^2 \sim 10$–$50$ GeV$^2$ while SLAC typically have $Q^2 \sim 2$ GeV$^2$ there. Shadowing may be invoked as the source of the considerable difference between the two experiments, but it is important to study the $Q^2$ behavior of the EMC effect for $x<0.2$ as precisely as possible and to determine the behavior of $\sigma_L/\sigma_L$ on nuclei.

(2) Experiments with neutrino beams[33] give results at variance with the EMC and SLAC data. The main discrepancy is again in the small-$x$ region where there is no evidence for an enhancement of the sea. One feature which must be cleared up is the precise shape of the structure function $F_2$ at small $x$ for $\nu$-iron interactions where present experiments[14,34] at high $Q^2$ differ significantly.

(3) Certain nuclei have "anomalous densities." That is, the density for some values of $A$ (e.g., $A=4$ or 48) deviate from a smooth behavior. It would be interesting to include such nuclei as $^3$He, $^6$Li, $^{48}$Ca to see if the nuclear-structure functions reflect this behavior. Figure 5 shows details of some of the "steps" in $F_2^A/F_2^{\rm D}$ which we expect because of the fluctuations in the nuclear density.

The central conclusion of this work is that there is evidence from experiment, through dynamical rescaling, that quarks are partially deconfined in dense nuclei and that the degree of deconfinement increases with atomic number. This may be the precursor to a deconfining phase transition at some higher density; it may even arise from a modification of symmetry-breaking dynamics which occurs in passing from the vacuum to nuclear matter.[35] There are a number of implications for several other hadronic processes that are immediately testable. One example is the nuclear dependence of lepton-pair production and of $J/\psi$ muoproduction.[36]

It may even turn out that structure functions for all hadrons are essentially determined by their sizes, a feature which then allows them to be related by a generalization of the rescaling relation.[37]

## ACKNOWLEDGMENTS

We wish to thank C. H. Llewellyn Smith, J. W. Negele, O. Nachtmann, H. Pirner, and A. W. Thomas for discussions and suggestions. R. L. Jaffe is indebted to the Science and Engineering Research Council, United Kingdom and the U. K. Theory Institute for partial support during this research. The work of R. L. Jaffe was supported in part through funds provided by the U.S. Department of Energy under Contract No. DE-AC02-76ER03069.

## APPENDIX A: DETERMINATION OF $\mu_A{}^2$

Following Ref. 8 we take $Q^2=\mu_A{}^2$ as the point where the bag calculation of matrix elements is appropriate and that the moments of the structure function $M_n^A(Q^2)$ at high $Q^2$ are obtained by evolving up in $Q^2$ according to the twist-two operators.

To determine $\mu_A{}^2$ we reverse this procedure and extrapolate the high-$Q^2$ behavior of the observed moments to low $Q^2$. We take the nonsinglet structure function $xF_3(x,Q^2)$ from the recent CERN-Dortmund-Heidelberg-Saclay (CDHS) data and compute the Nachtmann moments $M_n^{A=56}(Q^2)$. Note that the target for this experiment was iron. The $n=4,5,6$ moments can be reliably calculated in the range $5<Q^2<100$ GeV$^2$. According to the bag model the values of these moments $A_3^{\rm NS}(n,\mu_A{}^2)$ at $Q^2=\mu_A{}^2$ are 0.23, 0.14, and 0.10 for $n=4,5,6$. Plotting the quantity

$$\left[\frac{M_n^A(Q^2)}{A_3^{\rm NS}(n,\mu_A{}^2)}\right]^{-1/dn}=1+Y_n\ln(Q^2/\mu_A{}^2) \tag{A1}$$

versus $\ln Q^2$ yields a straight line, the value of $Q^2$ when the left-hand side $=1$ gives $\mu_A{}^2$. The plots are very good approximation to straight lines yielding

$$\left.\begin{aligned}\mu_A{}^2&=0.41\pm0.11\ \text{GeV}^2\ \ (n=4)\\ \mu_A{}^2&=0.53\pm0.11\ \text{GeV}^2\ \ (n=5)\\ \mu_A{}^2&=0.56\pm0.10\ \text{GeV}^2\ \ (n=6)\end{aligned}\right\}A=56\ . \tag{A2}$$

The mean value is $\mu_A{}^2=0.50\pm0.11$ GeV$^2$ for $A=56$. Taking the value of $\lambda_{A=56}/\lambda_{A=1}$ from Table I for a Reid soft-core correlation function, we get $\mu_{A=1}{}^2=0.66\pm0.14$ GeV$^2$.

## APPENDIX B: NEGLECT OF NINE-QUARK AND (HIGHER) CONFIGURATIONS

For two nucleons overlapping in the nucleus, $V_0$ the overlapping volume is used as the measure of six-quark bag formation, $P_6$. This idea can obviously be extended to obtain the probability for nine-quark bags from three-nucleon overlap. Let us look at a simple configuration which illustrates that the neglect of this last contribution may not be serious when estimating the confinement size, even when three-nucleon overlap is significant.

Take three spheres each of radius $a$, overlapping symmetrically each center distance $d$ from the other two. Our procedure is to compute the overlapping volume $V_0(d/a)$ between each pair [as given by Eq. (23)] and then, in this case, the ratio of the effective confinement radius $\lambda$ to the nucleon radius $\lambda_N$ is

$$\frac{\lambda_{\rm eff}}{\lambda_N}=1+2V_0(2^{1/3}-1)\ , \tag{B1}$$

where $V_0$ is calculated in units of the volume of one of the spheres. This is plotted as the solid curve in Fig. 6 as a function of the separation distance. If $\widetilde{V}_0(d/a)$ is the volume of overlap between all three spheres, then the contribution of nine-quark bags to $\lambda/\lambda_N$ is

$$\widetilde{V}_0(3^{1/3}-1) \tag{B2}$$

and is shown as the dotted curve in Fig. 6. Subtracting $\widetilde{V}_0$ from the two-sphere overlap volume $V_0$ gives the correct contribution of two-nucleon overlap,

$$2(V_0-\widetilde{V}_0)(2^{1/3}-1) \tag{B3}$$

which is shown as the dot-dashed curve in Fig. 6. The sum of (B1) and (B2) gives the net correct effect and is shown as the dashed line in Fig. 5.

The closeness of the solid and dashed curves gives us good reason to believe that the overestimate of the two-nucleon overlap is approximately compensated by our neglect of three-nucleon overlap—even when the latter is not small.

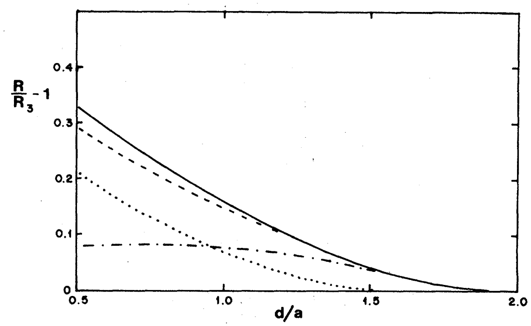


FIG. 6. Contributions to the effective confinement size for a symmetric three-nucleon system as a function of the separation $d$ between each pair scaled by the nucleon radius $a$. The solid curve is the result of neglecting three-nucleon overlap (our approach). The dot-dashed curve is the contribution from three-nucleon overlap and the dotted curve is the "true" two-nucleon overlap. The dashed curve is the sum of these two contributions.


[1]K. Rith, *Proceedings of the International Europhysics Conference on High Energy Physics, Brighton 1983*, edited by J. Guy and C. Costain (Rutherford Appleton Laboratory, Chilton, Didcot, United Kingdom, 1984), p. 80.

[2]J. J. Aubert *et al.* (EMC), Phys. Lett. **123B**, 275 (1983).

[3]A. Bodek *et al.*, Phys. Rev. Lett. **50**, 1431 (1983); **51**, 534 (1983).

[4]F. E. Close, R. G. Roberts, and G. G. Ross, Phys. Lett. **129B**, 346 (1983).

[5]R. L. Jaffe, Phys. Rev. Lett. **50**, 228 (1983).

[6]R. L. Jaffe, F. E. Close, R. G. Roberts, and G. G. Ross, Phys. Lett. **134B**, 449 (1984).

[7]R. G. Arnold *et al.*, Phys. Rev. Lett. **52**, 727 (1984).

[8]R. L. Jaffe and G. G. Ross, Phys. Lett. **93B**, 313 (1980).

[9]D. J. Gross, in *Proceedings of the XVIIth International Conference on High Energy Physics, London, 1974*, edited by J. R. Smith (Rutherford Laboratory, Chilton, Didcot, England, 1974), p. III-65.

[10]J. Negele (private communication).

[11]J. Negele (unpublished).

[12]F. Borkowski *et al.*, Nucl. Phys. **A222**, 269 (1974).

[13]A. Devoto, D. W. Duke, J. F. Owens, and R. G. Roberts, Phys. Rev. D **27**, 508 (1983).

[14]H. Abramowicz *et al.* (CDHS collaboration), Z. Phys. C **17**, 283 (1983).

[15]J. J. Aubert *et al.* (EMC), Phys. Lett. **123B**, 123 (1983).

[16]O. Nachtmann and H. J. Pirner, Z. Phys. C **21**, 277 (1984); Heidelberg Report No. HD-THEP-84-7, 1984 (unpublished).
[17]J. Dias de Deus, M. Pimenta, and J. Varela, Lisbon Report No. CFMC-E-1/84 (unpublished); Phys. Rev. D **30**, 697 (1984); Niels-Bohr Report No. NBI-HE-84-23, 1984 (unpublished).
[18]A. W. Hendry, D. B. Lichtenberg, and E. Predazzi, Phys. Lett. **136B**, 433 (1984).
[19]A. Krzywicki, Phys. Rev. D **14**, 152 (1976).
[20]N. N. Nikolaev Usp. Fiz. Nauk **134**, 369 (1981) [Sov. Phys. Usp. **24**, 531 (1981)].
[21]H. J. Pirner and J. Vary, Phys. Rev. Lett. **46**, 1376 (1981).
[22]C. E. Carlson and T. J. Havens, Phys. Rev. Lett. **51**, 261 (1983).
[23]C. H. Llewellyn Smith, Phys. Lett. **128B**, 107 (1983).
[24]M. Ericson and A. W. Thomas, Phys. Lett. **128B**, 112 (1983).
[25]E. L. Berger, F. Coester, and R. B. Wiringa, Phys. Rev. D **29**, 398 (1984).
[26]J. Szwed, Phys. Lett. **128B**, 245 (1983).
[27]Liu Feng, Li Jia-rong, and Liu Lian-Sou, Hua-Zhong Report No. HZPP-84-5, 1984 (unpublished).
[28]R. Voss, talk at Neutrino '84 meeting, Dortmund, 1984 (unpublished).
[29]J. J. Aubert, Phys. Lett. **105B**, 322 (1981).
[30]A. Bodek *et al.*, Phys. Rev. D **20**, 1471 (1979); M. D. Mestayer *et al.*, *ibid.* **27**, 285 (1983).
[31]J. F. Gunion, P. Nason, and R. Blankenbecler, Phys. Rev. D **29**, 2491 (1984); L. F. Abbott, E. L. Berger, R. Blankenbecler, and G. L. Kane, Phys. Lett. **88B**, 157 (1979).
[32]J. L. Cortéz, J. L. Miramontes, and J. Sanchez-Guillen, Phys. Rev. D **30**, 46 (1984).
[33]H. Abramowicz *et al.* (CDHS collaboration), Z. Phys. C **25**, 29 (1984); M. A. Parker *et al.*, Nucl. Phys. **B232**, 1 (1984); A. M. Cooper *et al.*, Phys. Lett. **141B**, 133 (1984).
[34]D. Macfarlane *et al.* (CCFRR collaboration), Report No. FERMILAB-Pub-83/108 (unpublished).
[35]L. S. Celenza, A. Rosenthal, and C. M. Shakin, Brooklyn Report No. BCINT 84/051/124k, 1984 (unpublished).
[36]F. E. Close and R. G. Roberts, Rutherford Appleton Report No. RAL-84-078, 1984 (unpublished).
[37]F. E. Close, R. G. Roberts, and G. G. Ross, Phys. Lett. **142B**, 202 (1984).